arXiv:cond-mat/0202097v1 [cond-mat.dis-nn] 6 Feb 2002

Retrieval and Chaos in Extremely Diluted Non-Monotonic Neural Networks

M. S. Mainieri and R. Erichsen Jr.

Instituto de Física, Universidade Federal do Rio Grande do Sul,

Caixa Postal 15051, CEP 91501-970, Porto Alegre, RS, Brazil

March 22, 2022

Abstract

We discuss, in this paper, the dynamical properties of extremely diluted, non-monotonic neural networks. Assuming parallel updating and the Hebb prescription for the synaptic connections, a flow equation for the macroscopic overlap is derived. A rich dynamical phase diagram, was obtained, showing a stable retrieval phase, as well as a cycle two and chaotic behavior. Numerical simulations were performed, showing good agreement with analytical results. Furthermore, the simulations give an additional insight into the microscopic dynamical behavior during the chaotic phase. It is shown that the freezing of individual neuron states is related to the structure of chaotic attractors.

1. Introduction

Models of neural networks have been largely studied since the pioneering work of Hopfield [1]. Assuming symmetric interactions and monotonic units, and using classical tools of statistical mechanics, equilibrium properties were extensively investigated. For a review in this subject, see, e. g., [2]. Nevertheless, the brain is a highly dynamical system, and equilibrium statistical mechanics should be not able to describe most of its properties. At our knowledge, the first work including the dynamical behavior as an important topic in neural networks research is due to Sompolinsky et al. [3]. In that work, it was shown that asymmetric synaptic connections between units, a plausible feature, results in cyclic and chaotic behavior in the network dynamics. The chaotic behavior in neural tissue is, in fact supported by biological observations [4].

More recently, a new class of models allowing for the complex behavior in neural networks started to be explored. It consists in networks of neurons in which the output activity is a non-monotonic function of the local input field. Next, we present a quick list with some important results available in the literature.

The feed-forward perceptron is an architecture where the main task to be performed is the classification of a set of input patterns. Following first step replica symmetry breaking calculations in the space of the synaptic interactions, see [5, 6] and references therein, the optimal capacity for classification of patterns is larger for the non-monotonic than for the monotonic perceptron. Still concerning this subject, non-monotonic perceptrons offer a further opportunity to study the fractal organization of the space of interactions [7].

In networks of recurrent architecture, the main subject concerns the associative memory property. If the dynamical evolution is governed by an hamiltonian, with the relaxation to an equilibrium distribution of states reproducing the process of memory retrieval. The question here is, if the dynamics is not governed by an hamiltonian, as in the case of non-monotonic, under which conditions it evolves to an equilibrium distribution of states keeping, in this way, the associative memory property? This problem was studied by Inoue [8], through the use of an equilibrium signal to noise analysis. It was found that, depending on the parameters defining the non-monotonicity, for binary patterns, and using the Hebb learning rule, the storage capacity, to be defined and discussed later, is highly improved, compared to monotonic neurons.

The dynamics of extremely diluted networks of continuous, non-monotonic neurons was studied in [9]. The associative memory property is still present, and a non-regular, chaotic-type attractor was also noticed. The authors pointed out the emergence of chaos as a consequence of the non-monotonicity. The categorization ability of extremely diluted, three-state, non-monotonic neural network was studied in [14, 15]. A categorization phase, as well as a chaotic phase, was noticed. In [11] there is a study of the chaotic attractors of a model with non-monotonic, binary neurons, with finite connectivity and binary synapses.

Our purpose in this paper is to study some of the dynamical properties of non-monotonic neural networks. The relaxation to the retrieval state, the appearing of oscillations and chaos, and the interplay between all these behaviors are discussed. In order to make transparent the essential physical aspects, the simplest model of non-monotonic neural network was chosen, i. e., the network of binary, reverse-wedge neurons, with hebbian connections. In order to have an analytically solvable dynamics, we restrict our study to the extremely diluted architecture with parallel updates. In addition, further insight on the microscopic dynamics during the chaotic phase, as well as in the transition from the chaotic to the retrieval phase, was obtained through numerical simulations.

2. Diluted network dynamics

We consider a network composed by N sites, whose state is represented by a set of variables $\{S_i\}$ $i = 1 \dots N$, with the state of the neuron in site i being represented by a binary variable $S_i = \pm 1$. In the absence of retrieval noise, each neuron updates in a synchronous, deterministic way according to

$$S_i(t+1) = F_\theta \left(h_i(t) \right) \ , \tag{1}$$

where

$$F_\theta(h) = \begin{cases} +1 & : \quad h < -\theta \ \text{ and } \ 0 < h < \theta \\ -1 & : \quad \text{otherwise} \end{cases} \tag{2}$$

is the reverse-wedge activation function. Here, θ is a threshold parameter. The local field felt by the neuron at site i is given by

$$h_i(t) = \sum_{i=1}^{N} J_{ij} S_j \ . \tag{3}$$

In the limit of extreme dilution each neuron is connected to C other neurons, with

$$1 \ll C \ll \ln N \, . \tag{4}$$

Due to this condition, the synaptic connections have a tree-like structure, and the existence of feedback-loops has a vanishing probability [9]. In consequence, the dynamics of this network is exactly solvable [12]. The storage capacity of the network is defined as $\alpha = p/C$. We assume that the synapses are given by a Hebb-like learning rule,

$$J_{ij} = \frac{C_{ij}}{C} \sum_{\mu=1}^{p} \xi_i^\mu \xi_j^\mu \, , \tag{5}$$

where C_{ij} are random binary variables assuming values 1, if the output of neuron j is connected to the input of neuron i and zero, otherwise. They are chosen according the probability distribution

$$P(C_{ij}) = \frac{C}{N} \delta(C_{ij} - 1) + \left(1 - \frac{C}{N}\right) \delta(C_{ij}) \, , \tag{6}$$

where $\delta(x)$ is the Dirac's delta function. The memories $\{\xi_i^\mu\}$, $i = 1 \ldots N$, $\mu = 1 \ldots p$ are a set of independent, identically distributed random binary variables, chosen according the probability distribution

$$P\left(\xi_i^\mu\right) = \frac{1}{2} \delta\left(\xi_i^\mu - 1\right) + \frac{1}{2} \delta\left(\xi_i^\mu + 1\right) \, . \tag{7}$$

The only relevant order parameters describing the macroscopic state of the network is the set of overlaps

$$m_\mu = \frac{1}{N} \sum_{i=1}^{N} \xi_i^\mu S_i \tag{8}$$

between the system configuration the stored patterns.

In what follows, we consider that only one memory pattern, say $\mu = 1$, has a macroscopic overlap of order $\mathcal{O}(1)$, and all the others $p-1$ are of order $\mathcal{O}(1/\sqrt{N})$. Following the now standard derivation of [12], we obtain that, in the absence of retrieval noise, the retrieval overlap satisfies the recursion relation

$$m_1(t+1) = -\frac{1}{2} \mathrm{erf}\left(\frac{m_1(t) + \theta}{\sqrt{2\alpha}}\right) + \frac{1}{2} \mathrm{erf}\left(\frac{m_1(t)}{\sqrt{2\alpha}}\right) - \frac{1}{2} \mathrm{erf}\left(\frac{m_1(t) - \theta}{\sqrt{2\alpha}}\right) \, . \tag{9}$$

For parallel dynamics, in the limit of extreme dilution, this equation fully describes the dynamical evolution of the network.

Before to extend the discussion for all θ, it worths to mention what is the behavior of the system in the limits $\theta \to \infty$ and $\theta \to 0$. For $\theta \to \infty$, the deterministic neuron update reduces to the signal transfer function $S_i(t+1) = \mathrm{sgn}[h_i(t)]$. The macroscopic dynamical evolution is given by $m(t+1) = \mathrm{erf}(m(t)/\sqrt{2\alpha})$. According to [12], this equation has a fixed-point for $t \to \infty$ at a finite value $m = m(\alpha)$, provided that $\alpha < 2/\pi$. At this value of the storage capacity, the system undergoes a continuous transition to the fixed point $m = 0$.

In the limit $\theta \to 0$, the neurons update according to the transfer function $S_i(t+1) = -\mathrm{sgn}[h_i(t)]$, with the macroscopic dynamics being given by $m(t+1) = -\mathrm{erf}(m(t)/\sqrt{2\alpha})$. This equation no longer have a finite fixed-point for finite m. Now, for small α, the network evolves dynamically through a cycle of length two, where the finite retrieval overlap changes from m to $-m$ from one time step to the other. In other words, in one time step, it retrieves one pattern, and in the next time step it retrieves the inverse of this pattern. The amplitude m of the limit cycle decreases continuously with the increasing α, arriving to $m = 0$ at the same storage capacity $\alpha = 2/\pi$ as in the previous case $\theta \to \infty$.

Now we start to discuss the long term behavior of the system. A complete dynamical phase diagram for general θ is shown in figure 1. In region I, corresponding to large α, the only fixed point of Eq. (9) is $m = 0$, known as the zero solution [10]. The region II, for intermediate and large θ, is the locus of the retrieval solution, with finite fixed point overlap $m \neq 0$. The transition between regions I and II is continuous. It worths to remark that the borderline for the retrieval region decreases monotonically from $\alpha = 2/\pi$ for large θ to $\alpha = 0$ for $\theta = 0$. This is in contrast to that reported by Inoue [8] for the fully connected network. There, the Hopfield limit $\alpha \approx 0.138$ is found for large θ. Then, decreasing θ, the borderline for the retrieval increases up to a maximum $\alpha \approx 0.211$ at $\theta \approx 1.77$. For smaller θ, it decreases till to reach $\alpha = 0$ at $\theta = 0$.

The region III is divided in two parts, one for small θ and $\alpha < 2/\pi$ and other close to the the θ axis, for $\theta < 1$. In this region, the network shows the cycle two behavior, as in the $\theta \to 0$ limit. The amplitude of the cycle two decreases monotonically to zero at the transition line between regions I and III. The transition from region III to other region than I is discontinuous.

In region IV the network has a periodic behavior. Leaving the retrieval re-

gion, roughly at the right and above, in the figure, it starts a period doubling cascade that ends in the chaotic region V.

Finally, we discuss the regions that are signaled with a star in figure 1. The star means that the long term behavior depends on the initial value m_0 of the overlap. If the initial value is sufficiently small, the network evolves to the basin of attraction of the corresponding phase without the star. Otherwise, it ends in the cycle two behavior, like in phase III.

3. Numerical simulations

The non-monotonic network with extremely diluted connections offers an interesting opportunity to compare microscopic and macroscopic views of non-linear phenomena. As an example, the bifurcation diagram of the overlap m for $\alpha = 0.04$ and varying θ is shown in figures 2a and 2b, determined, respectively from the macroscopic map of Eq. (9) and the microscopic definition of Eq. (8). The initial condition is $m_0 = 0.1$, i. e., outside the basin of attraction of the cycle two solution. Figure 2b results from simulation over a network with $N = 10000$ and $C = 100$. In order to save computer memory, only nonzero elements of the synaptic matrix where stored, as in [13]. Comparing the two diagrams, we can see that bifurcations and periodicity windows are less clearly defined in the simulation than in the macroscopic evolution. Furthermore, in the range in θ where states with $m > 0$ and $m < 0$ coexist in the same attractor, the diagram from simulation is more populated with states with small overlap. This is in contrast with the macroscopic evolution, that results in a more uniformly distributed diagram. We may ask if these discrepancies are due to the high connectivity value, since $C/N = 0.01$ in figure 2b, while figure 2a holds in the limit $C/N \to 0$. We believe that this is not the case, since simulations with $N = 1000$ and $C = 100$ give similar results. Instead of this, we believe that the discrepancies are due to finite size effects, since the definition $\alpha \equiv p/C$ holds for both p and C going to ∞ while, in the simulations we have $p = 4$. Nevertheless, although the discrepancies, there is a good general agreement between the two diagrams. In particular, the figures agree in which concerns to transitions from cyclic to chaos and to retrieval regions. This means that, even if Eq. (4) is not strictly satisfied, the simulations reproduce quite well the dynamics of the diluted network. With this, we conclude that it is justified to proceed with simulations, in order to obtain additional insight about the chaotic behavior of the network.

For completeness it is shown, in figure 2c, the Lyapunov exponent calculated from iterations of the macroscopic map (Eq 9). The positive values assumed confirm that the system displays a chaotic phase.

The description of the dynamical evolution through macroscopic variables leaves open some questions, mainly concerning the chaotic regime. We could ask, for instance, if the abrupt change in the overlap from step to step results from alternate flipping activity in all network sites, or if part of the sites are frozen and part are flipping. In order to have some insight about this and other questions, computational simulations were realized. Here we introduce, for each neuron i, the quantity $w_i(t) \equiv t - t_i$, where t_i is the time corresponding to the last flip of neuron i. Expressed in words, $w_i(t)$ is the number of time steps that neuron i stays in the same state, at time step t. Suppose that the network is in the cycle of period 2 with maximal amplitude. Then, all sites flip in each time step. In this case, $w_i = 0$ for all site i. Now suppose that, after to start, the network quickly arrives to an equilibrium state with all the neurons frozen in one state. In this case, after the time step t, all w_i are smaller but close to t. Between these two extreme, the distribution $P(w)$ gives a good picture of the dynamical state of the network.

The results for $P(w)$ are shown in figures 3a and 3b. To understand the figures, it is sufficient to know that if a neuron had its last flip n time steps before t, then it contributes with a count for $w = n$. The final time we adopted is $t = 500$, since this is a sufficient amount of time to reach the long-term behavior. Each figure results from an average over 50 runs. To take care of finite size effects, simulations were done for $N = 5000$ and $N = 10000$. Since the results were equivalent, they are shown only for $N = 10000$. We also have $C = 100$ and $p = 4$, so $\alpha = 0.04$. The initial condition is $m_0 = 0.1$. Different regions of the phase diagram were visited through changing θ. In figure 3a, $P(w)$ is shown for $\theta < 1.0$. The main feature to be extracted is that no freezing occurs: all neurons flip in a time interval smaller than 50 time-steps. For $\theta = 0.25$, the network in the region I* of the phase diagram, inside the basin of attraction of the zero phase. The condition $\theta = 0.3$ corresponds to a network in region II*, inside the basin of attraction of the retrieval phase, with a retrieval overlap $m \approx 0.1$ (see figure 2). Since the values of overlap involved are small, we could expect that part of neurons remains frozen, but this is in contrast to what actually happens. When $\theta = 0.7$, the network shows chaotic behavior. Since the chaotic attractor wanders through states with m going from large negative to large positive values (see figure 2b), we could expect, as it is confirmed, that all neurons have flipping activity. For

these three values of θ, $P(w)$ shows an exponential decaying behavior, with a similar decaying rate. Results for $\theta = 0.9$ is also included in figure 3a. Now we observe a distinct behavior, with $P(w)$ decaying more slowly than in the previous cases. We guess that this is already a consequence of the dynamical transition that occurs at a slightly higher θ value, where the chaotic attractor splits in two, one for $m > 0$ and other for $m < 0$, as can be seen in figure 2b.

The plot of $P(w)$ for $\theta = 1.0$, $\theta = 1.2$ and $\theta = 1.3$ is shown in figure 3b. For $\theta = 1.0$, the system is in phase V, just above the θ value where the chaotic attractor splits in two. The decaying is slower than exponential, but there are not frozen sites. We conclude that the splitting in the chaotic attractor is not related to the freezing of a part of sites. Rather, it is related to a change in the decaying rate in $P(w)$ that allows for an important decrease in the flipping activity. When $\theta = 1.2$, the network is in the periodic regime of phase IV, with positive overlap. The flipping activity decreases, as reveals the small population for $w \approx 0$, and an important concentration of frozen sites can be seen for large w. In view of this, we may state that the appearing of a periodic retrieval regime with positive m is related to the freezing of part of the neurons. It worths to note that $P(w)$ shows a nontrivial structure for $w > 300$. We don't know, at this moment, how to explain this structure. Finally, for $\theta = 1.3$ the system is in retrieval regime. The figure shows a small population for small w corresponding to sites that are flipping. There is a range for intermediary w with zero or very small population, and a large population for large w, corresponding to frozen sites. Since the retrieval overlap $m \approx 0.93$ is large, we conclude that most of sites are frozen in the direction of the pattern.

4. Conclusion

Following a dynamical approach, we have studied the extremely diluted non-monotonic neural network. The results show that there is no improvement in the storage capacity of the retrieval phase due to the non-monotonicity: it is always smaller than that of the network with monotonic neurons. As stated above, this is in contrast with the highly connected network [8]. There, an optimal θ, whose storage capacity is larger than that of the monotonic network, was observed. It would be interesting to study a network with finite connectivity, ranging from zero, that is the present model, to 1, that is the highly connected model. In this way, it would be possible to localize where

is the changeover from one regime to the other.

Numerical simulations were performed in order to get additional information about the microscopic dynamical evolution. The quantity observed was the amount of time that each neuron i is fixed without flip, w_i. Excluding the trivial cycle-two regime for $\theta < 0.2$, where $P(w) \approx \delta(w)$, the distribution $P(w)$ shows three distinct regimes, depending on the flipping activity of the network: high flipping activity with exponential decaying $P(w)$, mean flipping activity with less than exponential decay, and low flipping activity with freezing.

We conclude that the distribution $P(w)$ gives a good picture of the microscopic evolution of the network, in its different dynamical regimes. It was not the aim of this paper, but in a future work it could be interesting to investigate quantitatively the decaying law in the second regime.

Acknowledgements

The authors thank Dr. W. K. Theumann, Dr. M. A. P. Idiart, Dr. F. A Tamarit and Dr. N. Lemke for fruitful discussions. M. S. M. thanks CNPq (Conselho Nacional de Desenvolvimento Cientfico e Tecnolgico - Brazil) for financial support.

References

[1] J. J. Hopfield, *Proc. Nat. Acad. of Sci.* **79** 2554 (1982).

[2] J. Hertz, A. Krogh and R. G. Palmer, *Introduction to the theory of Neural computation*. Reading: Addison Wesley, 1991.

[3] H. Sompolinsky, A. Crisanti and H. J. Sommers, *Phys. Rev. Lett.* **61** 259 (1988).

[4] A. Babloyantz, J. M. Salazar and C. Nicolis, *Phys. Lett.* **111A** 152 (1985).

[5] G. Boffetta, R. Monasson and R. Zecchina *J. Phys. A: Math. Gen.* **26** L507 (1993).

[6] D. Bollé and R. Erichsen Jr. *J. Phys. A: Math. Gen.* **29** 2299 (1996).

[7] R. Monasson and D. O'Kane *Europhys. Lett.* **27** 85 (1994).

[8] J. Inoue *J. Phys. A: Math. Gen.* **29** 4815 (1996).

[9] D. Bollé, B. Vinck and V. A. Zagrebnov, *J. Stat. Phys.* **70**, 1099 (1993).

[10] D. Bollé, G. M. Shim, B. Vinck and V. A. Zagrebnov, *J. Stat. Phys.* **74**, 565 (1994).

[11] D. Caroppo, M. Manarelli, G. Nardulli and S. Stramaglia *Phys. Rev. E* **60** 2186 (1999)

[12] B. Derrida, E. Gardner, and A. Zippelius, *Europhys. Lett.* **4**, 167 (1987).

[13] J. J. Arenzon, N. Lemke, *J. Phys. A: Math. Gen.* **27**, 5161 (1994).

[14] D. R. C. Dominguez and W. K. Theumann, *J. Phys. A: Math. Gen.* **30**, 1403 (1997).

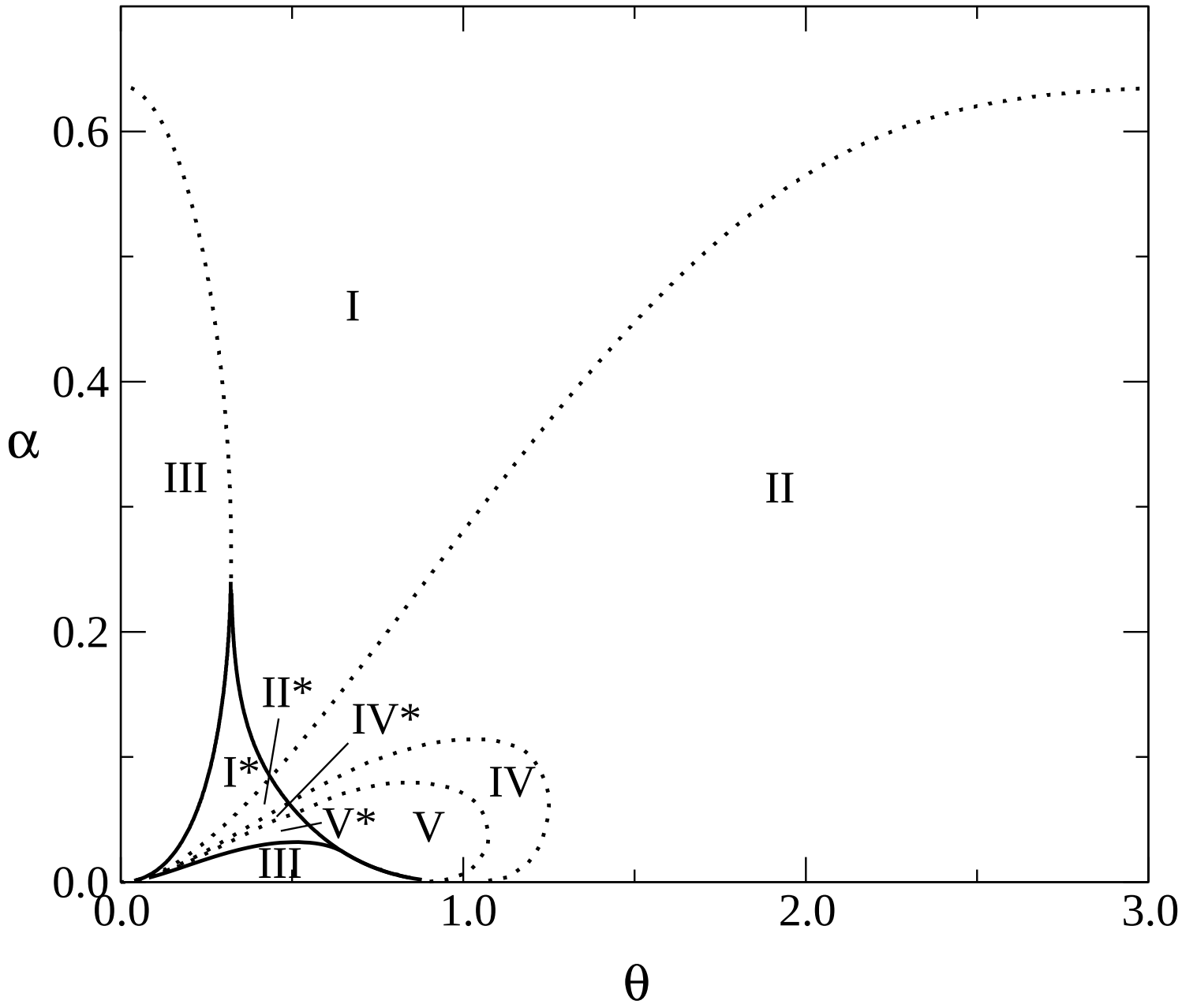
[15] D. R. C. Dominguez, *Phys. Rev. E* **54**, 4066 (1996).

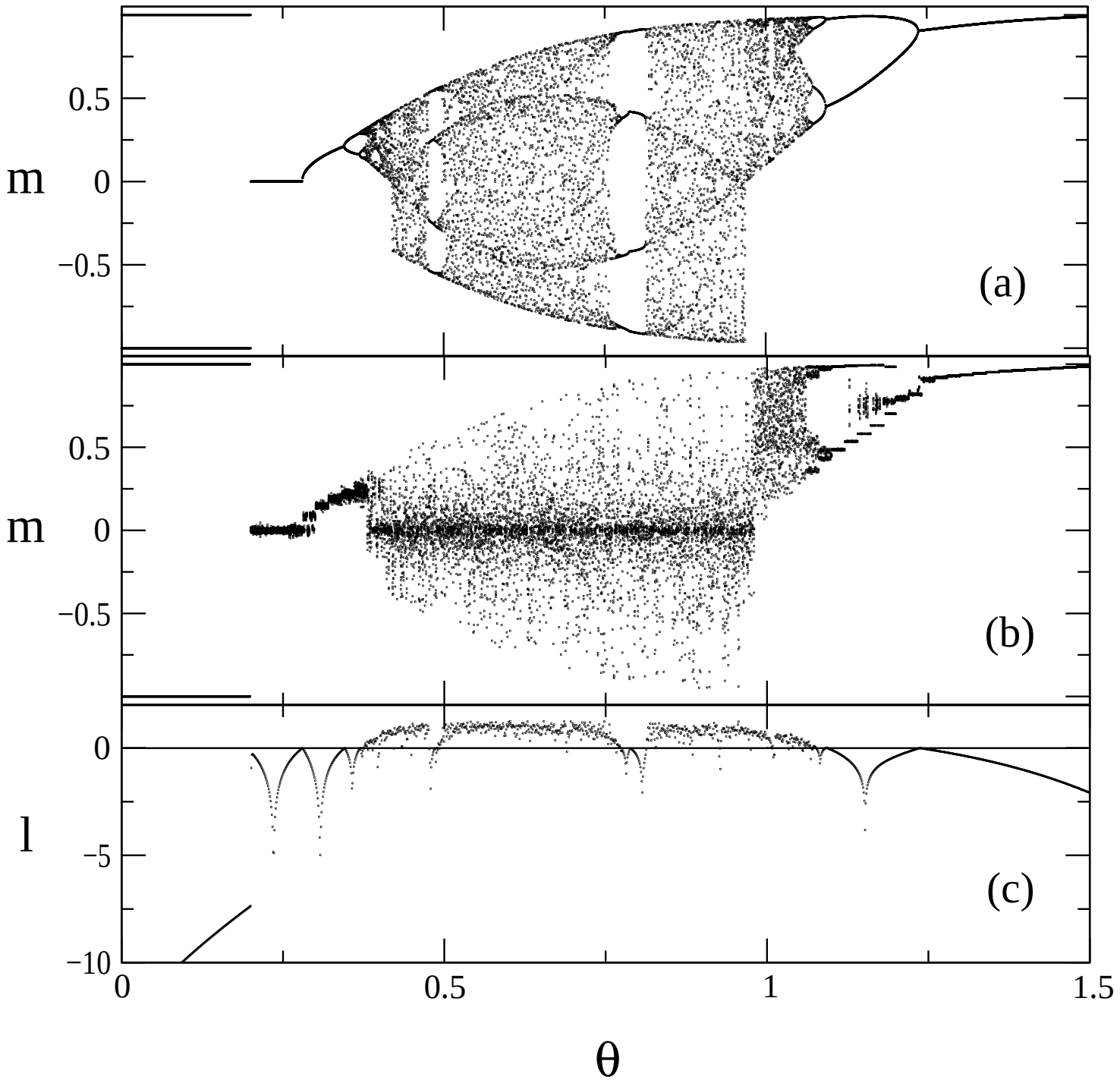
Figure Captions

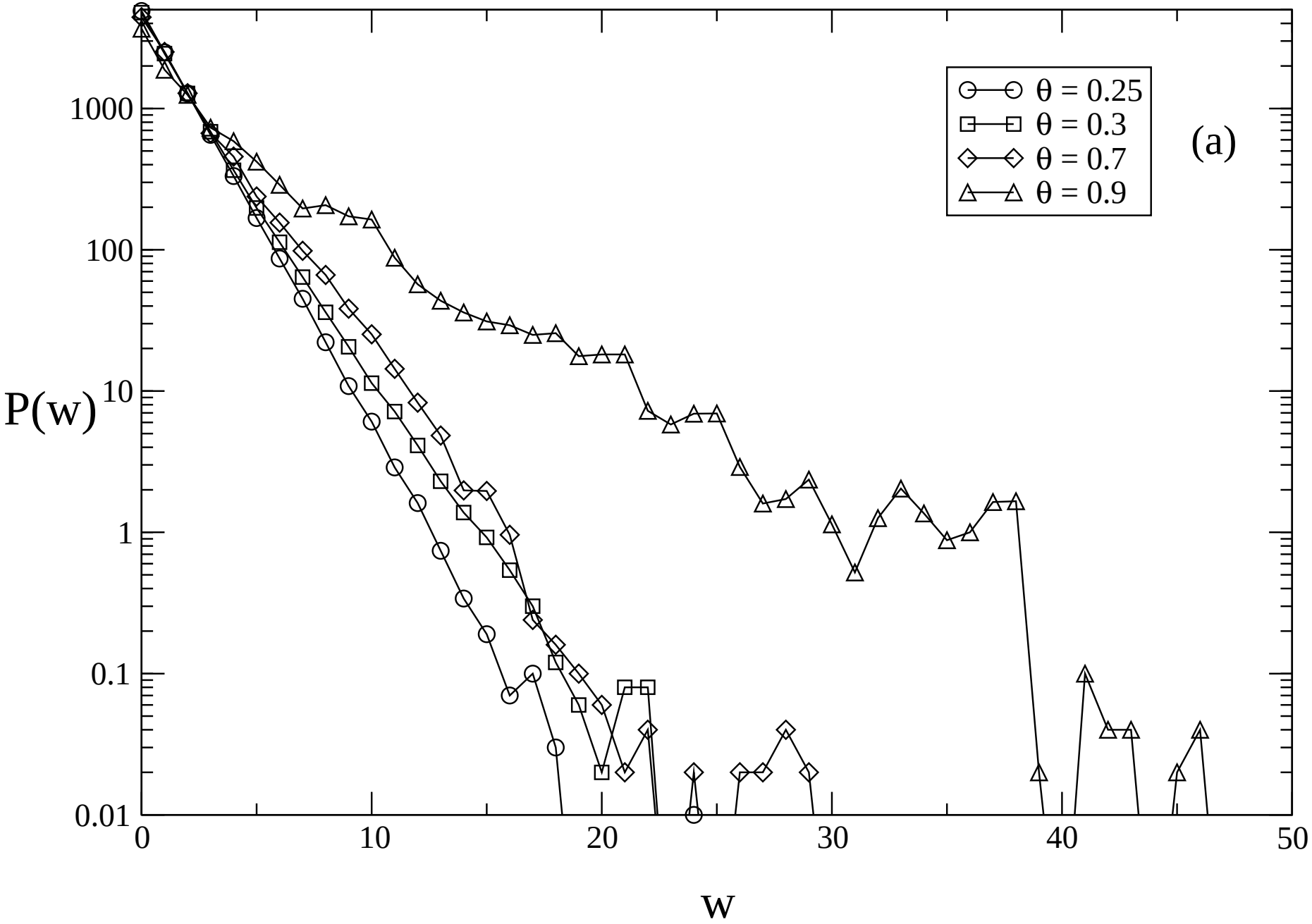
Figure 1: Phase diagram for the extremely diluted non-monotonic neural network. Solid (dotted) lines correspond to discontinuous (continuous) phase transitions. For the dynamical behavior in each phase, see the text.

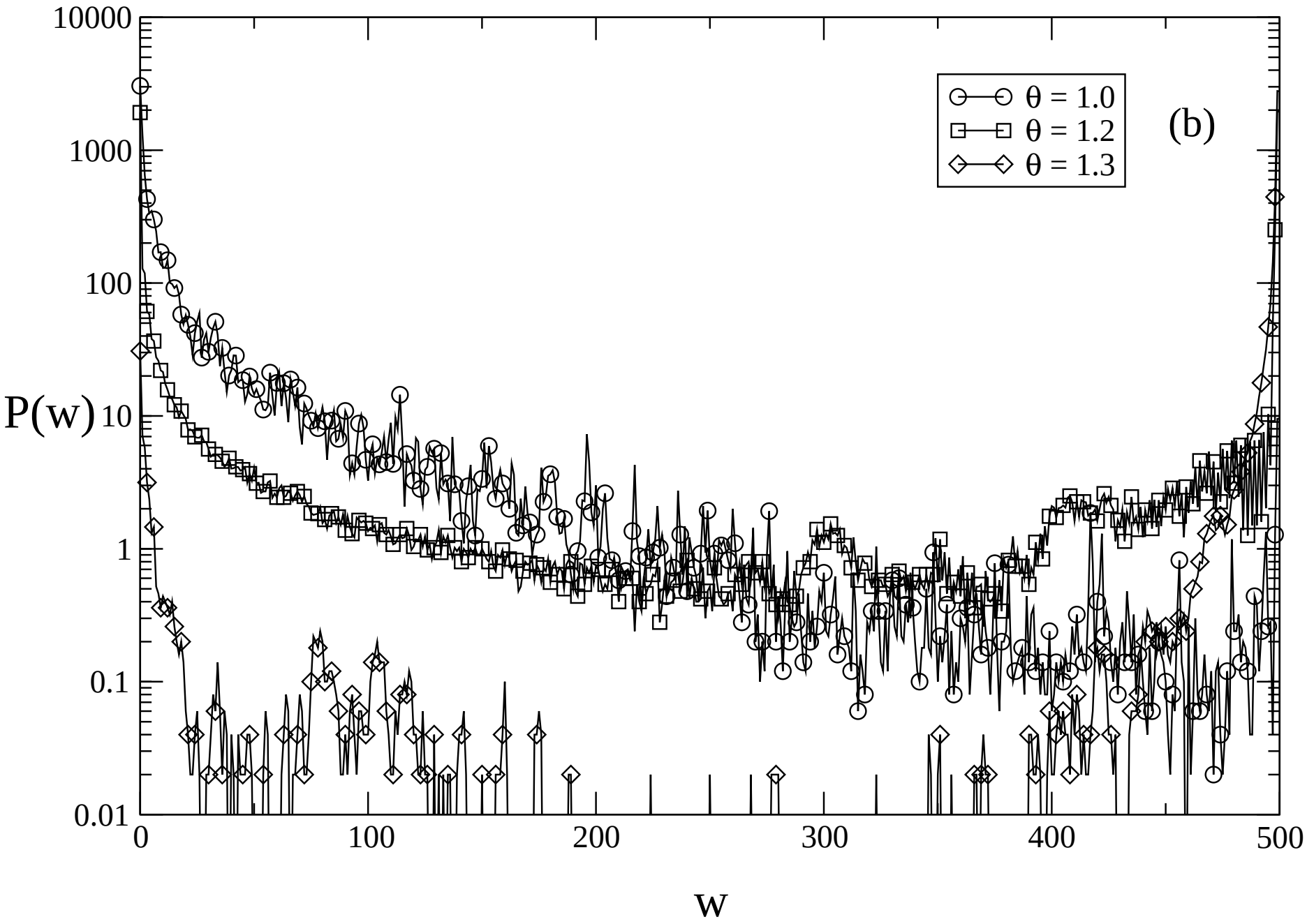
Figure 2: Bifurcation diagram and Lyapunov exponent for the extremely diluted non-monotonic neural network, for $\alpha = 0.04$ and varying θ, with the initial condition $m_0 = 0.1$. (a) Bifurcation diagram obtained from iteration of Eq. (9); (b) bifurcation diagram obtained from simulation in a network with 10000 neurons, computing the overlap in each time step from its definition in Eq. (8); (c) Lyapunov exponent, obtained from the iteration of Eq. (9).

Figure 3: Distribution $P(w)$ for the extremely diluted non-monotonic neural network, for $\alpha = 0.04$, after simulations with 10000 neurons. (a) threshold θ in the range 0.25 – 0.9; (b) threshold θ in the range 1.0 – 1.3


0.6
0.4
0.2
0.0
α
0.0
1.0
2.0
3.0
θ
I
II
III
II*
IV*
I*
IV
V*
V
III


m
0.5
0
−0.5
(a)
m
0.5
0
−0.5
(b)
l
0
−5
−10
(c)
0
0.5
1
1.5
θ


θ = 0.25
θ = 0.3
θ = 0.7
θ = 0.9
(a)
P(w)
w
1000
100
10
1
0.1
0.01
0
10
20
30
40
50


10000
1000
100
10
1
0.1
0.01
P(w)
0
100
200
300
400
500
w
θ = 1.0
θ = 1.2
θ = 1.3
(b)